Dopant-atom-based Tunnel SOI-MOSFETs

M. Tabe,[1] D. Moraru,[1] E. Hamid,[1] A. Samanta,[1]
L. T. Anh,[2] T. Mizuno,[1] and H. Mizuta[2,3]

[1]Research Institute of Electronics, Shizuoka University
3-5-1, Johoku, Naka-ku,
Hamamatsu 432-8011, Japan
[2]Japan Advanced Institute of Science and Technology,
Nomi, Japan
[3]School of Electronics and Computer Science, University
of Southampton, United Kingdom

Introduction

Recently, dopant-induced fluctuation of device characteristics has been recognized as one of the most serious problems for further progress of CMOS technology [1]. On the other hand, as an extreme limit of MOSFETs, FET characteristics influenced by a single-dopant atom were reported from several groups [2-5], where carrier transport mechanism is tunneling through individual dopant atoms. In this background, we have proposed and demonstrated *dopant-atom devices* from a different viewpoint to the CMOS technology trend, i.e., single-dopant (SD) transistors [5], SD memories [6], SD turnstiles [7-9] and SD photonic devices [10-12]. In those devices, only one or a few dopants are intentionally used in the channel and one dopant works as a quantum well for electron (or hole) tunneling transport.

P-donor atom in nanoscale channels of SOI-MOSFETs

When we focus on a phosphorous (P) donor atom, it can be treated as a hydrogen-like atom in Si matrix. Based on the effective mass approximation, the ionization energy, or the binding energy, of the donor atom with respect to the Si conduction band minimum is as small as 45 meV. Therefore, P-atom tunneling devices can operate only at low temperatures below ~20 K, since at high temperatures electrons are thermally excited and tunneling transport mechanism does not work. However, when a dopant is embedded in Si nanostructures, its electronic states are significantly different from those in bulk Si, and its ionization energy is predicted to be enhanced due to effects of dielectric and quantum size confinement [13].

Most recently, we have demonstrated high-temperature operation of donor-atom MOSFETs at around 100 K because of donor state deepening in specifically-designed nano-stub-channels, as shown in Figs. 1 and 2 [14]. Such progress toward room temperature operation is critical for practical application of "atom devices". These results are qualitatively evidenced by *ab initio* atomistic simulations of individual dopants in Si nanostructures. More details, including observation of single dopants by low-temperature Kelvin probe force microscopy (LT-KFM) [15-18], will also be presented.

References

[1] S. Roy and A. Asenov, Science **309**, 388 (2005).
[2] H. Sellier *et al.*, Phys. Rev. Lett. **97**, 206805 (2006).
[3] G. P. Lansbergen *et al*., Nature Phys. **4**, 656 (2008).
[4] Y. Ono *et al.*, Appl. Phys. Lett. **90**, 102106 (2007).
[5] M. Tabe *et al.*, Phys. Rev. Lett. **105**, 016803 (2010).
[6] E. Hamid *et al.*, Appl. Phys. Lett. **97**, 262101 (2010).
[7] D. Moraru *et al.*, Phys. Rev. B **76**, 075332 (2007).
[8] D. Moraru *et al.*, Appl. Phys. Express **2,** 071201 (2009).
[9] K. Yokoi *et al.*, J. Appl. Phys. **108**, 053710 (2010).
[10] M. Tabe *et al*., Phys. Status Solidi A **208** , 646 (2011).
[11] A. Udhiarto *et al.*, Appl. Phys. Lett. **99**, 113108 (2011).
[12] A. Udhiarto *et al.*, Appl. Phys. Express **5**, 112201 (2012).
[13] M. Diarra *et al*., Phys. Rev. B **75**, 045301 (2007).
[14] E. Hamid *et al.*, Phys. Rev. B **87**, 085420 (2013).
[15] M. Ligowski *et al.*, Appl. Phys. Lett. **93**, 142101 (2008).
[16] M. Anwar *et al.*, Appl. Phys. Lett. **99** , 213101 (2011).
[17] M. Anwar *et al.*, Jpn. J. Appl. Phys. **50,** 08LB10 (2011).
[18] R. Nowak *et al.*, Appl. Phys. Lett. **102**, 8, 083109 (2013).

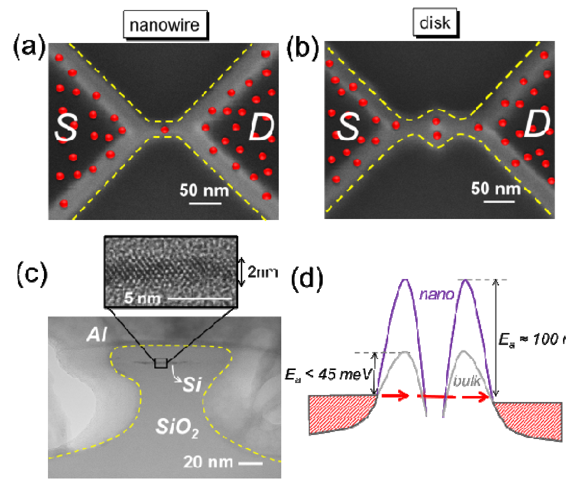

Fig. 1. (a)-(b) Top-view SEM images with schematic dopant distribution and outlined boundaries for the two channel patterns investigated: non-stub [(a)] and stub [(b)]. (c) Cross-sectional TEM image across the channel area, with a zoom-in on the ultrathin Si channel. (d) Expected change of a donor tunnel barrier height in nanostructures, as compared to bulk Si.

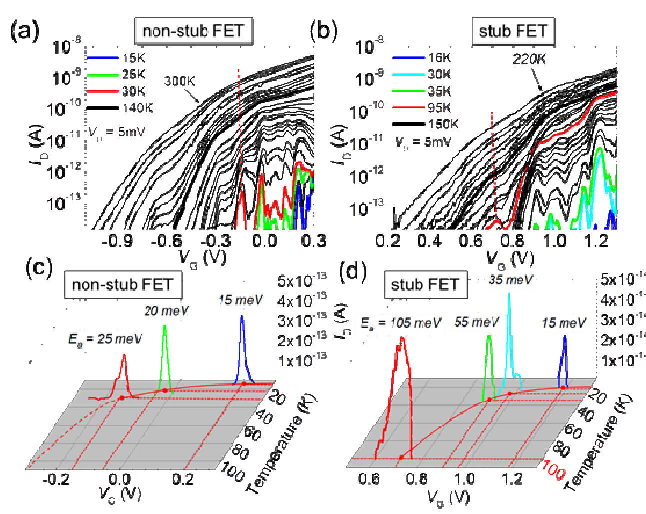

Fig. 2. (a)-(b) I_D-V_G characteristics for representative devices of each type: with a non-stub-channel [(a)] and with a stub-channel [(b)]. (c)-(d) From the data shown above, only the final emerging current peaks, at the lowest V_G, are shown, as a function of both V_G and temperature (T).